11th International Renewable Energy Storage Conference, IRES 2017, 14-16 March 2017, Düsseldorf, Germany

Power fluctuations in solar-storage clusters: spatial correlation and battery response times

James Barry*, Nina Munzke, Jorge Thomas

Karlsruhe Institute of Technology, Hermann-von-Helmholtz-Platz 1, 76344 Eggenstein-Leopoldshafen, Germany

Abstract

Well-designed and intelligently controlled battery storage systems are crucial for the successful integration of solar photovoltaic systems. The power variations in densely clustered systems such as those in residential areas could either be mitigated by small batteries in each household or by a district-scale storage solution. In this context it is useful to understand the correlation between individual array power outputs as a function of the distance between them. The study of correlation length and storage system response time provides a basis for optimal system design, depending on the context. Although it has already been shown that for a typical household storage system in Germany a dead time of 5 seconds in the control loop would lead to an small but non-negligible economic effect, in off-grid systems with 100% renewable energy supply the effects would be more dramatic, since the voltage and resulting power quality depends on the rapid response of the storage system to variations in power input. In order to characterise these effects the fluctuations in power output from 68 spatially separated photovoltaic arrays (each with 10 kWp) installed on the north campus of Karlsruhe Institute of Technology were analysed in detail with high-frequency data. This analysis was used to create virtual clusters of photovoltaic systems with different separation distances that were then used as inputs to a 32 kWh storage system on site. The effect of response time is studied by employing two sensors of different sampling rates. This allows one to quantify the resulting power smoothing due to both correlation effects and battery control algorithms, thus providing a benchmark for storage system integration in the local context.

Keywords: solar power fluctuations; correlation; storage systems; battery response time

1. Introduction

The variable nature of renewable energy sources necessitates mitigation technologies capable of fast response times. Battery energy storage systems combined with power electronics and communication and control infrastructure are one of the leading candidates for this role, in particular when it comes to compensating fluctuations on short time scales. Large-scale deployment of such systems, mostly with Li-ion battery technology [1], is currently under way, and will ultimately allow a greater penetration of renewable energy on the grid.

---

* Corresponding author. Tel.: +49-721-608-28287 ; fax: +49-721-608-28284.
  E-mail address: james.barry@kit.edu

In general, solar photovoltaic (PV) plants display particularly large and fast changes in power output, with extreme ramp rates occurring relatively often. The non-Gaussian statistics of the cloud-induced fluctuations in solar irradiation have been studied before [2–4]: it has been shown that power ramp rates of up to 60% of peak power per second are possible [5], but that the aggregation of multiple solar plants leads to a smoothing effect. Several models have sought to characterise the spatio-temporal correlations of solar power variability in different contexts (see for example Refs. [5–9]). Simply put, it has been shown [6,9–12] that the further apart the individual solar arrays are, the less correlated the variations in power output become, and that this reduction in correlation is less pronounced for larger time increments.

However, apart from Ref. [12] and the recent analysis [4] using a spatially dense network of radiation sensors, there are few studies focussing on very short time scales and distances, largely due to a lack of relevant data. To this end, the authors performed a basic statistical analysis [13] of power fluctuations from the 1 MW solar park at Karlsruhe Institute of Technology (KIT), which forms the basis for this work. Data collected over one year with a resolution of 1 Hz was analysed for fluctuation correlations at short time scales. The presence of battery systems on site provides the ideal framework to examine the effects of these correlations in the storage context.

In residential areas, the power variations in densely clustered solar PV systems could either be mitigated by small batteries in each household or by a district-scale storage solution. In the case of smaller or off-grid systems the effects of very short-term fluctuations become important and can affect power quality, due to voltage flicker, for example. Although decorrelation between arrays can help to mitigate these effects, the integration of a battery storage system allows further control over ramp rates, thus facilitating higher PV penetration. Experience with prototype storage systems has shown that in order to successfully smooth PV fluctuations one needs control algorithms with a cycle time on the order of one fifth of a second or better.

Control systems always possess a certain amount of latency, which leads to unwanted power flows. A recent simulation [14] showed that for a household storage system in Germany, a dead time of 5 seconds in the control loop would lead to a monetary loss of roughly €15 per annum. However in reality these effects could be larger and should be studied in an experimental setup. In off-grid systems with 100% renewable energy supply the effects would be more noticeable, since the voltage and power quality depends on the rapid response of the storage system to variations in power input.

The effects of both spatial correlation and battery response times are examined in what follows. Using the results of Ref. [13], data from two array pairs with different correlations coefficients are selected as inputs for an AC-coupled storage system equipped with current sensors of different sampling rates. This unique installation allows for the comparison of control speed as well as a closer examination of spatially-induced correlation effects. In the next section, a brief description of the PV and battery installations is given, as well as an outline of the test procedure (more details of the correlation analysis can be found in Ref. [13]). The test results are presented in Section 3, and we summarise and conclude in Section 4.

Nomenclature

$\rho_{ij}^{\Delta t}$	array pair correlation: two-point correlation coefficient between time series of power increments ΔP_i and ΔP_j, for the time interval Δt
ΔP_i	power increments for array i
$P_{\mathrm{PV}}^{1(2)}$	PV power measured by sensor 1 (2)
$P_{\mathrm{batt}}^{1(2)}$	battery power measured by sensor 1 (2)
P_{residual}	residual power, difference between load target and sum of battery and PV power

---

2. Methodology

2.1. The 1 MW PV installation

Figure 1 depicts the layout of the "static solar-tracking configuration" 1 MWp PV installation at KIT, which has been described in more detail in Refs. [13,15]. There are six different PV module types making up 102 separate arrays

of roughly 10 kW each, installed at a variety of inclination and orientation angles, and four inverter types (labelled A...D) connect the arrays to the institute grid, as summarised in Table 1. The distance between the centre points of any two arrays ranges from 7.4 m to 251.6 m.

Table 1. Array numbers by orientation (rows), inclination (columns) and inverter type, where types A, B, C, D are green, magenta, blue and red, respectively.

	2°	15°	30°	45°	60°
60° E		1, 2	3, 4	5, 6	7, 8
45° E		9, 10, 11	12, 13	14, 15	16, 17
30° E		18, 19, 20, 21, 22, 23	24, 25	26, 27, 28	29, 30, 31
15° E		32, (33), 34	35, 36, (37)	38, 39, 40	41, 42, 43
00° (S)	46, 47, 48	(44), 45	49 , 50 51 52, 53, 54	55, 56	57, 58
15° W		59, 60, 61	62, 63, 64	65, 66, (67)	(68), 69, 70
30° W		71, 72, 73, 74, 75, 76	77, 78, 79	(80), 81, 82	83, 84, 85
45° W		86, 87, 88	89, 90	91, 92	93, 94
60° W		95, 96	97, 98	99, 100	101, 102

2.2. The 32 kWh AC-coupled storage system

An AC-coupled Li-ion battery storage system with 32 kWh capacity is installed in an air-conditioned container next to the 1 MW PV field. The battery is connected via a bi-directional inverter with a rated power of 30 kW to the AC-grid. The system topology is shown in Fig. 2: the central control unit is responsible for collecting measurement signals from each of the system components and executing control algorithms that ultimately set a charge or discharge target power for the battery. There are two current sensors of different sampling rates that measure the AC power generated by the PV system as well as that flowing to or from the battery, providing four different power signals, as shown in Table 2. Since the battery is essentially independent of the PV array, it is possible to run the battery control algorithm with different sources for the PV power profile, i.e., either with real data from one of the 10 kW PV arrays or else with a "virtual" PV input signal.

Table 2. Power values measured by the two different AC current sensors.

	Sensor PV(1)	Sensor PV(2)	Sensor Batt(1)	Sensor Batt(2)
Measured quantity	P_{PV}^1	P_{PV}^2	P_{batt}^1	P_{batt}^2
Sampling rate	≤ 50 Hz	1 Hz	≤ 50 Hz	1 Hz

2.3. Analysis of fluctuation correlations

The original fluctuation analysis was carried out using DC power data collected over the 2015 calendar year from 68 PV inverters of type A with a sampling rate of 1 Hz. After discarding the night time values and normalising the power time series, the correlation matrices $\rho_{ij}^{\Delta t}$ of array pair correlations between the time series of power increments ΔP_i and ΔP_j were calculated for different time intervals Δt and arrays i and j (see Ref. [13] for details of the calculation procedure).

Figure 3 provides a graphical representation of the 68×68 symmetric correlation matrix for different time scales, where the inverters are ordered by their number (cf. the green numbers in Table 1 – this is equivalent to an ordering by orientation, see also Fig. 5). Roughly speaking, one can observe that correlation increases with time scale and distance, since small distances are represented by elements close to the diagonal of the matrix. The effect of shadowing can also be seen - a number of arrays show very little correlation with the others, even at large time scales.
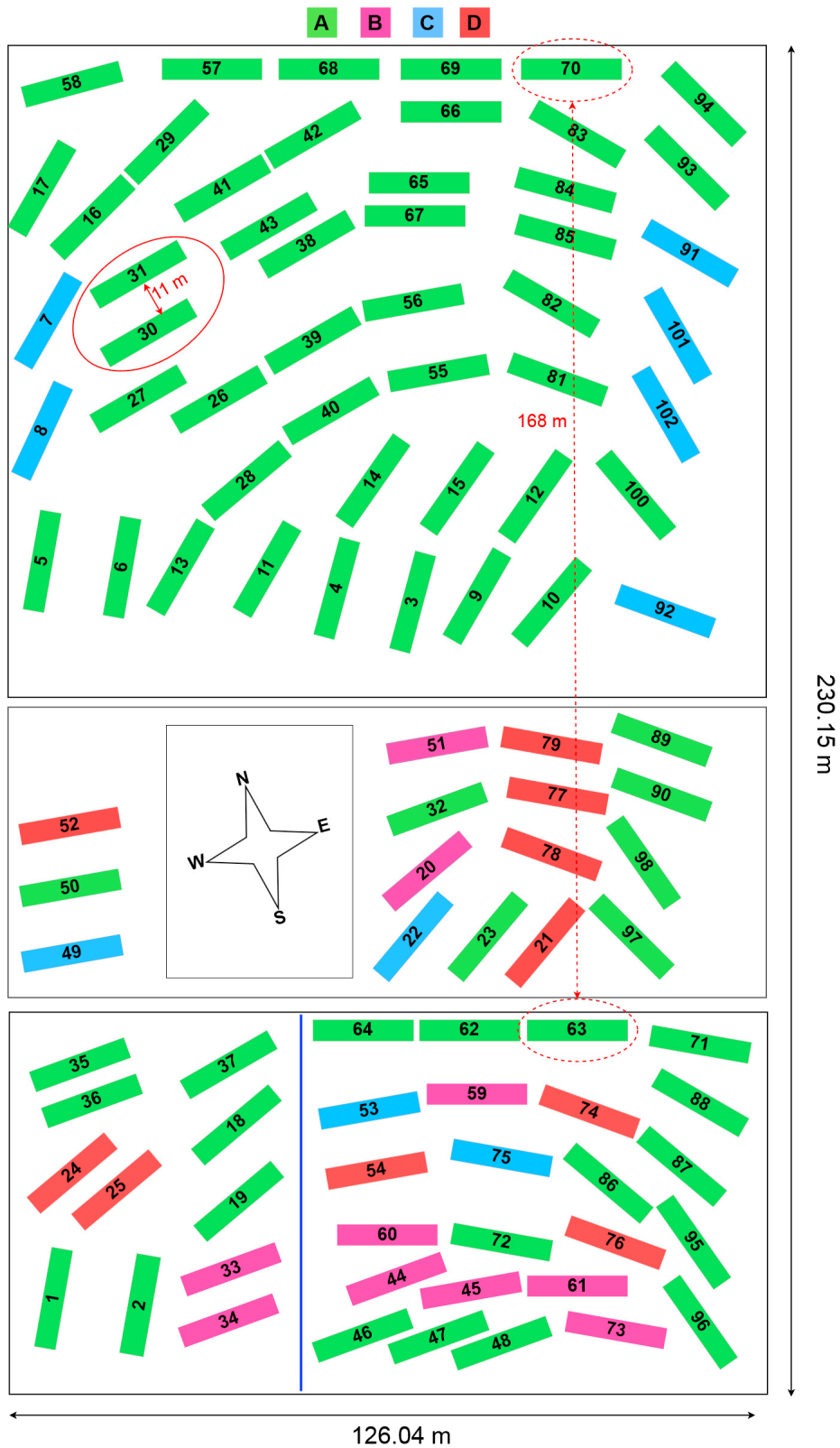
Fig. 1. Schematic diagram of PV field layout, with array numbers and colours corresponding to those in Table 1. The two array pairs with high (low) correlation coefficients are circled with solid (dashed) red lines, and the distance between them is indicated by the arrows (see Section 2.3).
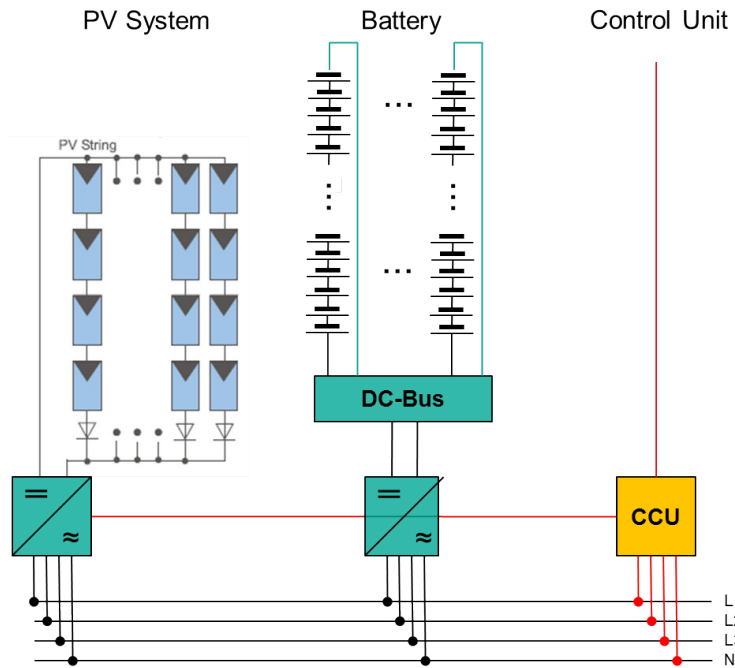
Fig. 2. Schematic diagram of the AC-coupled system, with power (communication) networks denoted by black (red) lines.
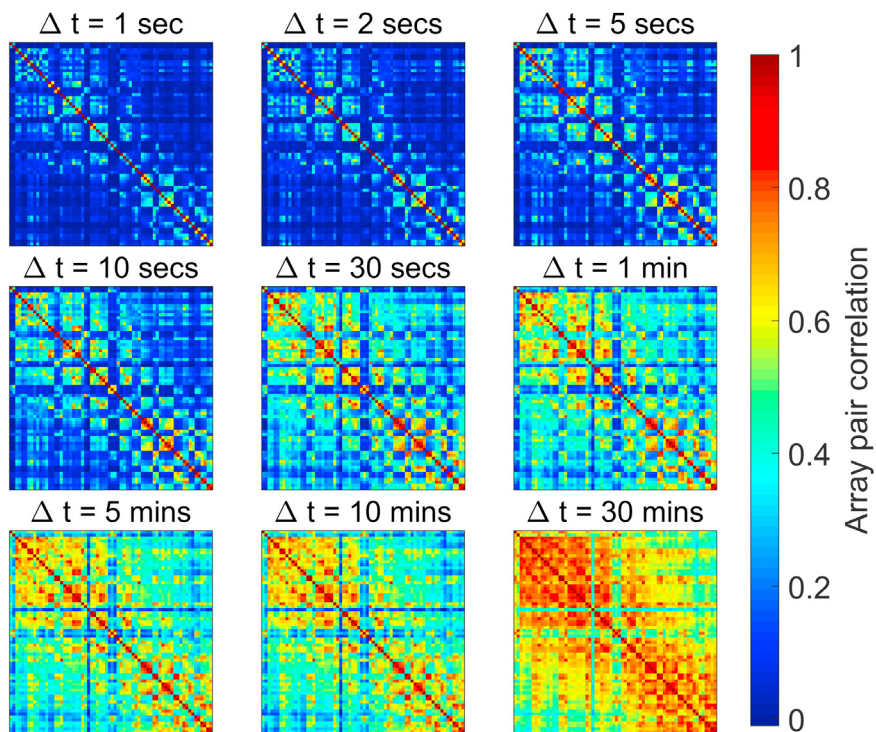

Fig. 3. Fluctuation correlation matrix at different time scales, using power time series data from 68 inverters of type A.
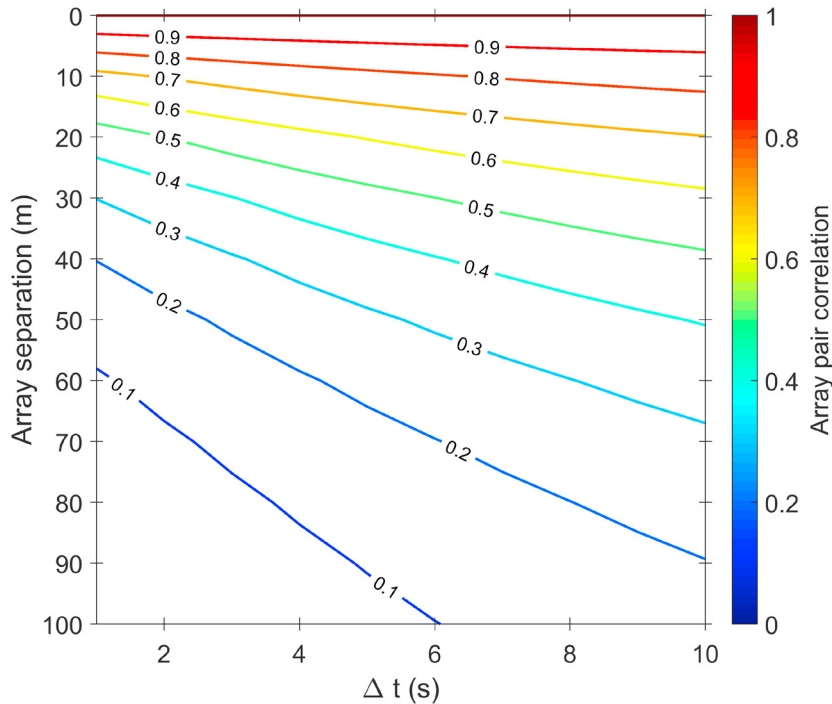
Fig. 4. Contour plot of correlation as a function of array separation and time scale, using power time series data from 68 inverters of type A and the exponential model in Eq. (1).

The relationship between distance and correlation at different time scales can be studied by fitting the measured data with an exponential model [7,9], i.e.,

$$\rho_{ij}^{\Delta t} = \exp\left(\frac{d_{ij}\ln(0.2)}{1.5\,\Delta t\,v_2}\right),$$ (1)

where d_{ij} is the separation between array i and j, and v_2 is a parameter representing the cloud speed. The results are shown in the contour plot in Fig. 4, for time scales from 1 to 10 seconds. This allows one to read off the minimal distance required for a certain level of decorrelation, for instance in order to reduce correlation to $\rho_{ij} = 0.2$ for 5 second fluctuation time increments, one should place the PV arrays at least 62 m apart. Note that these results depend on the local conditions, since fluctuations are dependent on the characteristics of the climatic zone, which influences the value of the parameter v_2 [9].

In order to examine the effect of orientation and inclination more closely, it is useful to order the inverters by either orientation or inclination angle, as in Fig. 5, where the correlation matrix for fluctuations of 5 seconds has been ordered in two different ways. In both plots one observes that in general the arrays closer to the diagonal have higher correlation factors, simply because their separation d_{ij} is lower. The plot on the left shows that orientation also plays a role: two arrays both facing east or west are more correlated with each other than a combination of one facing east and one facing west, as is to be expected. The plot on the right shows that a large proportion of the arrays inclined at 60° are correlated with each other, more so than for any other inclination angle.

2.4. Solar-storage cluster simulation

In the storage system context it is useful to focus on fluctuations of 5 seconds, since typical battery storage systems have response times of this order of magnitude. The analysis of fluctuation correlations is applicable in the context of storage system design, since one can get a rough idea of the smoothing effects of aggregating several
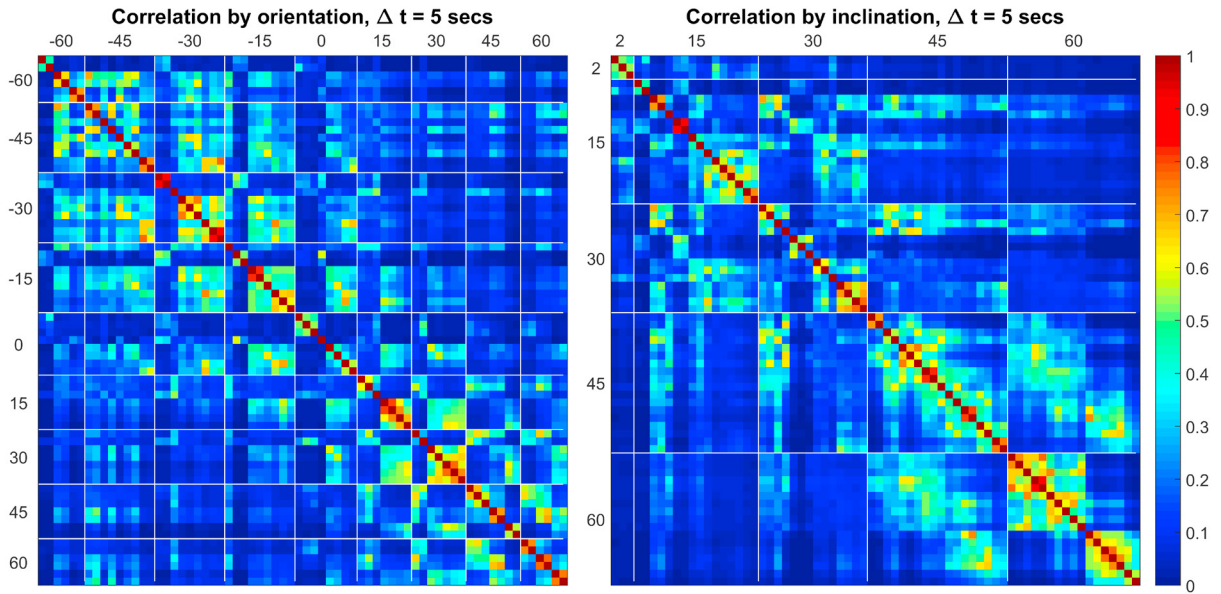
Fig. 5. Correlation matrix for fluctuations of 5 seconds, ordered by array orientation (left) and inclination (right) respectively. The orientation angles are defined with respect to south, where negative (positive) values represent the easterly (westerly) direction.

PV arrays in a mini-grid, for instance. As an example of this, normalised power curves from array 63 and 70 ($\rho_{63-70}^{\Delta t=5s} \simeq 0.074$, $d_{63-70} \simeq 168\,\mathrm{m}$) are shown in the left panel of Fig. 6, along with their average, for a three minute period of large cloud-induced fluctuations on 26 April 2015, whereas the right panel contains data from array 31 and 30 ($\rho_{31-30}^{\Delta t=5s} \simeq 0.86$, $d_{31-30} \simeq 11\,\mathrm{m}$). Here one can see that the combined power P_{PV}^{low} (left panel) shows a less dramatic fluctuation per installed kWp than P_{PV}^{high} (right panel), simply because the cloud reaches the arrays at different times. The short pause of roughly 12 seconds could help the battery system to catch up; since most storage systems on the market have a response time of anywhere between 5 and 15 seconds [16] this may or may not be enough to help smooth the fluctuations.

In order to examine this effect more closely, two hours of data from the morning of 13 April 2015 was used as an input to the AC-coupled storage system described in Section 2.2 above. Two different PV curves were created by adding the normalised powers of array 63 and 70 (P_{PV}^{low}) and array 31 and 30 (P_{PV}^{high}), and the result was scaled to have a peak power of 15 kW (see Fig. 7). It is evident that these data represent an extreme case with large fluctuations. The system was programmed to follow the load curve shown in Fig. 8, which is part of an example day taken from the VDI load profiles in the category ÜWH ("Übergang, Woche, Heiter"), i.e. a mostly clear weekday in spring or autumn. This fits with the PV data above, since one can see that although the number of fluctuations are large (characteristic of the fast-moving clouds experienced in April in Germany), the prevailing weather conditions were in a sense "clear" due to the high peak power measured from the PV arrays. In order to better match the energy consumption and generation over the course of the day, the load profile was scaled to 4.5 times its original size.

2.5. Test procedure

In order to compare the response of the two different sensor types as well as the effects of fluctuation correlations, the AC-coupled system was given the load profile in Fig. 8 as its power setpoint (P_{load}^{target}), with the two different PV profiles in Fig. 7 as the input power. The control algorithm then uses the battery to make sure that the system follows the required demand curve, i.e.,

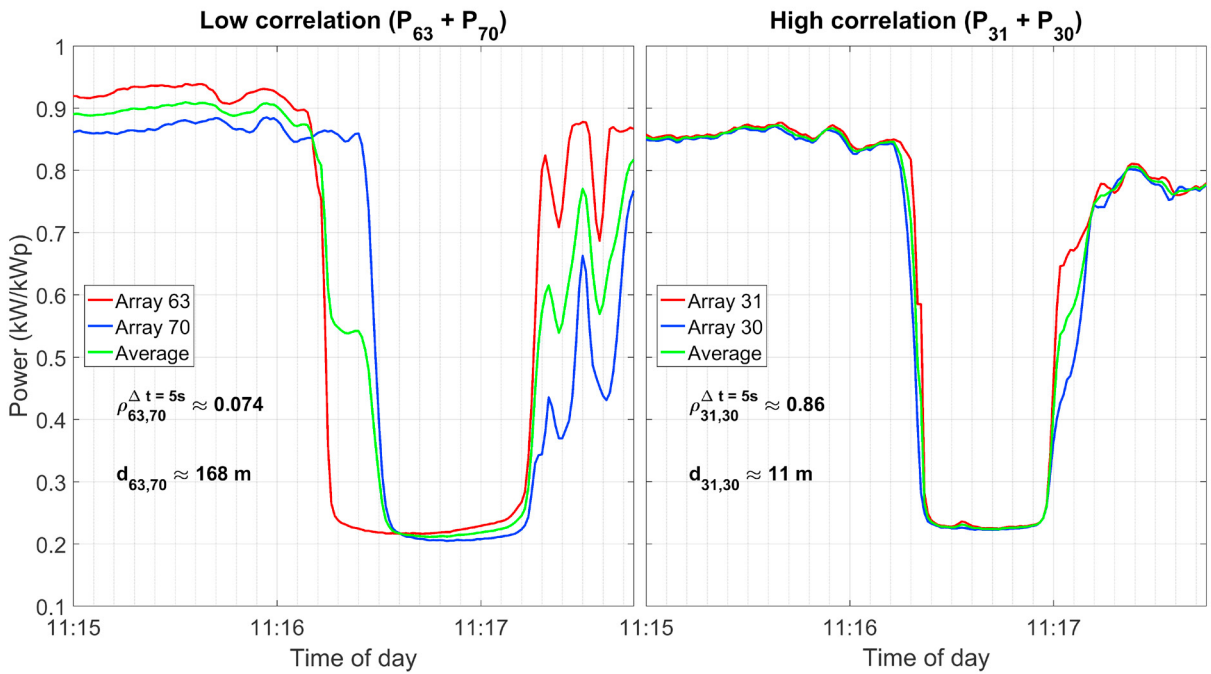$$P_{batt}^{target} = P_{load}^{target} - P_{PV}^{1(2)}, \tag{2}$$

Fig. 6. Comparison of power data from three minutes on 26 April 2015 for two different array pairs with different correlation coefficients and separation distances.
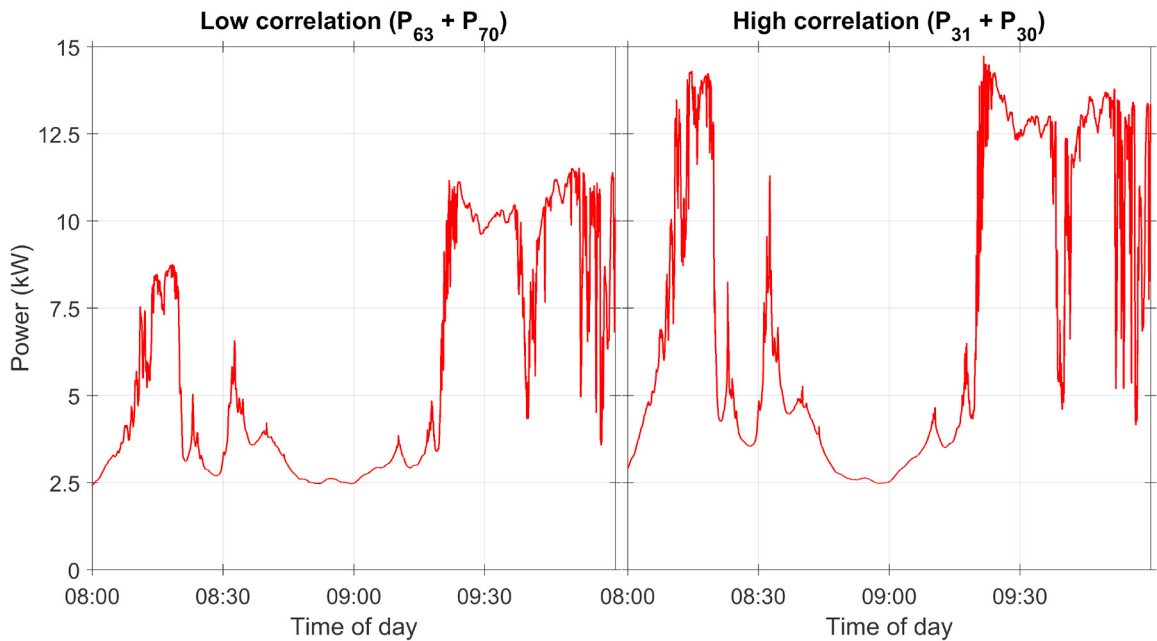
Fig. 7. PV power profiles measured on the morning of 13 April 2015, from two different array pairs with low (left panel) and high (right panel) correlation coefficients, see also Fig. 6.
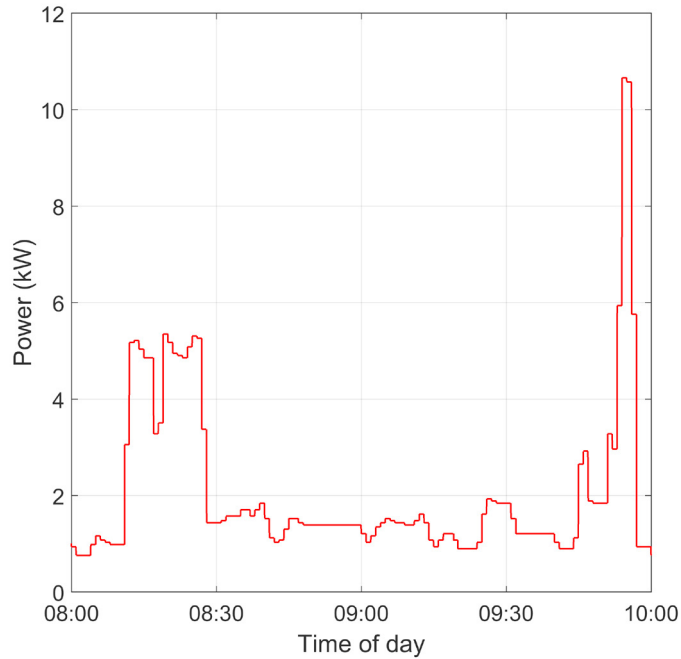
Fig. 8. Example load profile from the VDI standard, category ÜWH (see text for explanation).

where $P_{\text{load}}^{\text{target}}$ is the VDI load shown in Fig. 8 and $P_{\text{PV}}^{1(2)}$ is the PV profile shown in Fig. 7 and measured by sensor 1(2) respectively (cf. Table 2). The process variable input to the control loop is given by $P_{\text{batt}}^{1(2)}$ in each case. An additional derating routine ensures that the charge (discharge) current and resulting power is reduced once the battery is full (empty). The tests were performed with sampling frequencies of 5 Hz for sensor 1 and 1 Hz for sensor 2, for both PV and battery powers, respectively.[1]

3. Results and discussion

The effects of fluctuations in load and generation profiles as well as battery response times depend largely on the context in which the storage system is deployed. In general the variations in load are more prominent and faster than those in the generated PV power. Indeed, in the grid-connected context one would expect the load-induced fluctuations to play the major role [16], but considering the prevalence of extreme PV fluctuations it is reasonable that both be taken into account. In the household scenario the main result of slow control algorithms is firstly a reduction in self-sufficiency, since the grid is often called upon to make up the shortfall due to slow response times. At the same time one also feeds more energy into the grid if the battery is too slow to take it up, which decreases self-consumption ratio but may increase revenue from feed-in tariffs, if these exist.

Since the test described above did not include an explicit load, one can simply calculate a residual power

$$P_{\text{residual}} = P_{\text{PV}}^{1(2)} + P_{\text{batt}}^{1(2)} - P_{\text{load}}^{\text{target}}, \tag{3}$$

---

[1] Although sensor 1 can operate at an internal frequency of 50 Hz, the external control algorithm only changed the setpoint and process variable at a rate of 5 Hz.
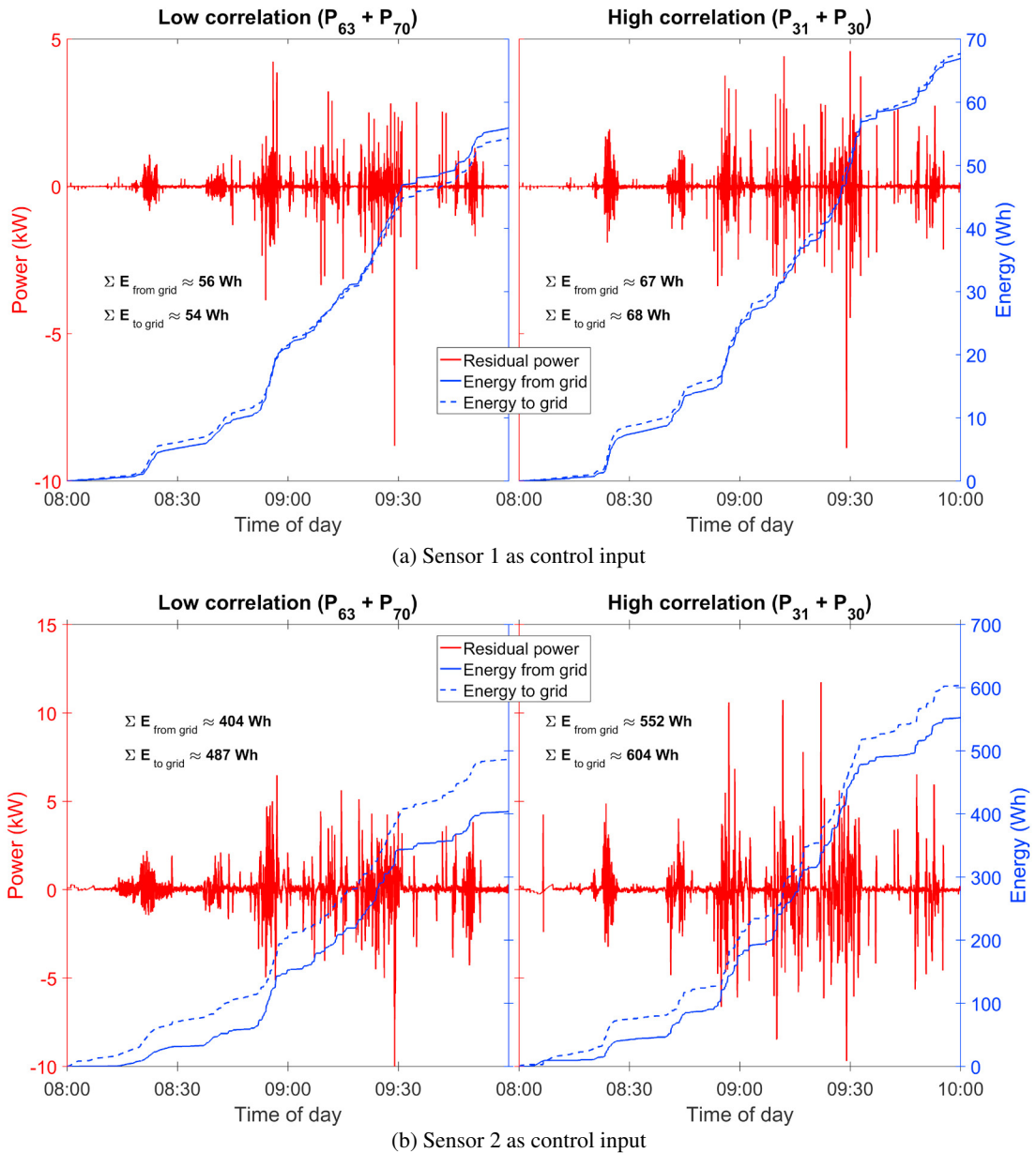
Fig. 9. Residual power (difference between actual and target power at the grid), as well as energy deficit (energy from grid) and surplus (energy to grid) that results from a finite response time.

which is the difference between the measured and target power produced at the "load" or strictly speaking at the grid. If $P_{residual} > 0$, excess power is fed into the grid, whereas if $P_{residual} < 0$, power is drawn from the grid to make up the deficit.

The results in Fig. 9 show that the effect of slow measurement and response time far outweighs the effects of correlation. For the case of low correlation, the slower sensor (left panel of Fig. 9b) resulted in on average 446 Wh of unwanted energy flows in either direction in the space of two hours, whereas the faster sensor (left panel of Fig. 9a) only leads to an average of 55 Wh drawn from and fed into the grid in the same time interval. On the other hand, the

highly correlated data (see the right panels of Fig. 9) shows on average 68 kWh (578 kWh) of unwanted energy flows for sensor 1 (sensor 2), which means that the decorrelation effect decreases the residual energy by roughly 18% (23%) for sensor 1 (sensor 2), respectively. Further studies will be performed with more input data, in order to verify this effect, since the data shown here represent a period of large fluctuations.

4. Summary and Conclusions

The study of variations in PV power over short time scales provides useful information for the design of storage systems with renewable energy, especially in cases where several PV arrays are installed close together (on the order of tens of metres). In cases where a central storage unit is installed, knowledge of the decorrelation length of characteristic cloud-induced fluctuations allows one to determine the appropriate battery response times. Correlations between fluctuations at different time scales can lead to a reduction in the overall frequency of fluctuations, which in turn reduces the requirements for mitigation. Battery systems designed to compensate variations in solar power (and other renewable energy sources) need to be able to respond within a few seconds to fast changes in power. In the specific example shown here, the decorrelation effect was shown to improve the system's overall energy efficiency over a two hour period by roughly 20%, however, far more important to a system's ability to provide renewable energy consistently is the response time of the control loop. Reducing the sampling rate from 5 Hz to 1 Hz led to nearly a tenfold increase in unwanted energy flows, which in the household context leads to a concomitant decrease in self-sufficiency and self-consumption ratios.

Further studies with different load profiles and larger volumes of data will provide further insights into the preliminary results presented here. The correlation effects depend both on season and climate, so that one could try to develop a model for different parts of the world (see also Ref. [9]). As emphasised before: the off-grid context provides the more interesting test of such correlation effects, since here the voltage and power quality depends to a large extent on the ability of the system to mitigate fluctuations. One would also expect such a mini-grid to contain closely spaced PV arrays, so that the unique mixture of PV-battery installations at KIT provides a good benchmark for real world scenarios.

Acknowledgements

References

[1] Sauer, D.U.. Lithium-ion batteries become the benchmark for stationary applications Markets, players, prices, technology. In: 10th International Renewable Energy Storage Conference. Düsseldorf: Eurosolar; 2016,.

[2] Marcos, J., Marroyo, L., Lorenzo, E., Alvira, D., Izco, E.. Power output fluctuations in large scale pv plants: One year observations with one second resolution and a derived analytic model. Progress in Photovoltaics: Research and Applications 2011;19(2):218–227. URL: http://dx.doi.org/10.1002/pip.1016. doi:10.1002/pip.1016.

[3] Anvari, M., Lohmann, G., Wächter, M., Milan, P., Lorenz, E., Heinemann, D., et al. Short term fluctuations of wind and solar power systems. New Journal of Physics 2016;18(6):1–14. URL: http://dx.doi.org/10.1088/1367-2630/18/6/063027. doi:10.1088/1367-2630/18/6/063027.

[4] Lohmann, G.M., Monahan, A.H., Heinemann, D.. Local short-term variability in solar irradiance. Atmospheric Chemistry and Physics 2016;16(10):6365–6379. URL: http://www.atmos-chem-phys.net/16/6365/2016/. doi:10.5194/acp-16-6365-2016.

[5] Lave, M., Kleissl, J., Arias-Castro, E.. High-frequency irradiance fluctuations and geographic smoothing. Solar Energy 2012;86(8):2190–2199. URL: http://dx.doi.org/10.1016/j.solener.2011.06.031. doi:10.1016/j.solener.2011.06.031.

[6] Hoff, T.E., Perez, R.. Quantifying PV power Output Variability. Solar Energy 2010;84(10):1782–1793. URL: http://dx.doi.org/10.1016/j.solener.2010.07.003. doi:10.1016/j.solener.2010.07.003.

[7] Hoff, T.E., Perez, R.. Modeling PV fleet output variability. Solar Energy 2012;86(8):2177–2189. URL: http://dx.doi.org/10.1016/j.solener.2011.11.005. doi:10.1016/j.solener.2011.11.005.

[8] Lave, M., Kleissl, J., Stein, J.S.. A wavelet-based variability model (WVM) for solar PV power plants. IEEE Transactions on Sustainable Energy 2013;4(2):501–509. URL: http://dx.doi.org/10.1109/TSTE.2012.2205716. doi:10.1109/TSTE.2012.2205716.

[9] Remund, J., Calhau, C., Perret, L., Marcel, D.. Characterization of the spatio-temporal variations and ramp rates of solar radiation and PV. Tech. Rep. IEA-PVPS Task 14, Subtask 1.3; International Energy Agency Photovoltaic Systems Programme; 2015. URL: http://iea-pvps.org/index.php?id=95&eID=dam_frontend_push&docID=2733.

[10] Marcos, J., Marroyo, L., Lorenzo, E., Alvira, D., Izco, E.. From irradiance to output power fluctuations: the PV plant as a low pass filter. Progress in Photovoltaics: Research and Applications 2011;19(5):505–510. URL: http://doi.wiley.com/10.1002/pip.1063. doi:10.1002/pip.1063.

[11] Perpinan, O., Marcos, J., Lorenzo, E.. Electrical power fluctuations in a network of DC/AC inverters in a large PV plant: Relationship between correlation, distance and time scale. Solar Energy 2013;88:227–241. URL: http://dx.doi.org/10.1016/j.solener.2012.12.004. doi:10.1016/j.solener.2012.12.004.

[12] Elsinga, B., van Sark, W.. Spatial power fluctuation correlations in urban rooftop photovoltaic systems. Prog Photovolt: Res Appl 2014;23:1390–1397. URL: http://dx.doi.org/10.1002/pip.2539. doi:10.1002/pip.2539.

[13] Barry, J., Munzke, N., Thomas, J.. Short-Term Power Fluctuations in Densely Clustered PV-Battery Systems. In: 32nd European Photovoltaic Solar Energy Conference and Exhibition. 2016, p. 2393 – 2398. URL: https://www.eupvsec-proceedings.com/proceedings?fulltext=barry&paper=37815. doi:10.4229/EUPVSEC20162016-6CO.12.2.

[14] Weniger, J., Tjaden, T., Bergner, J., Quaschning, V.. Auswirkungen von Regelträgheiten auf die Energieflüsse in Wohngebäuden mit netzgekoppelten PV-Batteriesystemen. In: 31. Symposium Photovoltaische Solarenergie. 2016,URL: http://pvspeicher.htw-berlin.de/wp-content/uploads/2014/04/WENIGER-2016-Auswirkungen-von-Regeltr%C3%A4gheiten-auf-die-Energiefl%C3%BCsse-in-Wohngeb%C3%A4uden-mit-netzgekoppelten-PV-Batteriesystemen.pdf.

[15] Thomas, J., Munzke, N.. A Static Solar-Tracking Configuration for PV Power Plant to Redistribute the Daily Power Supply. In: 31st European Photovoltaic Solar Energy Conference and Exhibition. 2015,URL: http://www.eupvsec-proceedings.com/proceedings?paper=33024.

[16] Munzke, N., Barry, J., Schwarz, B.. Performance Evaluation of Household Li-Ion Battery Storage Systems. In: 32nd European Photovoltaic Solar Energy Conference and Exhibition. 2016, p. 1516 – 1521. URL: https://www.eupvsec-proceedings.com/proceedings?fulltext=barry&paper=38157. doi:10.4229/EUPVSEC20162016-5AO.9.5.